Drag-driven instability of a dust layer in a magnetized protoplanetary disc

RAA 2016 Vol. **16** No. **9**, 134 (8pp) doi: 10.1088/1674–4527/16/9/134
http://www.raa-journal.org *http://iopscience.iop.org/raa*

***R**esearch in*
***A**stronomy and*
***A**strophysics*

Drag-driven instability of a dust layer in a magnetized protoplanetary disc

Mohsen Shadmehri[1], Razieh Oudi[2] and Gohar Rastegarzade[2]

[1] Department of Physics, Faculty of Sciences, Golestan University, Gorgan 49138-15739, Iran; *m.shadmehri@gu.ac.ir*
[2] Department of Physics, Semnan University, Semnan 35196-45399, Iran

Received 2015 July 21; accepted 2016 May 3

Abstract We study drag-driven instability in a protoplanetary disc consisting of a layer of single-sized dust particles which are coupled to the magnetized gas aerodynamically and the particle-to-gas feedback is included. We find a dispersion relation for axisymmetric linear disturbances and growth rate of the unstable modes are calculated numerically. While the secular gravitational instability in the absence of particle-to-gas feedback predicts the dust layer is unstable, magnetic fields significantly amplify the instability if the Toomre parameter for the gas component is fixed. We also show that even a weak magnetic field is able to amplify the instability more or less irrespective of the dust-gas coupling.

Key words: instabilities — protoplanetary discs

1 INTRODUCTION

Although the outer parts of protoplanetary discs are prone to gravitational instability, the inner parts are stable with respect to gravitational perturbations (e.g., Rafikov 2005). It is known that the onset of gravitational instability in an accretion disc occurs when the Toomre parameter becomes less than a threshold value around unity and the survival of the newly formed fragments is guaranteed when the cooling time-scale is less than a few dynamical time-scales (e.g., Gammie 2001). Although *dissipationless* gravitational instability is able to explain some of the observational features of structure formation in protoplanetary discs (e.g., Matzner & Levin 2005), the presence of dust particles can introduce new physical mechanisms that allow dust particles to clump together so that larger objects that may eventually grow into planetary embryos (e.g., Chiang & Youdin 2010). This is mainly because of the interactions between dust particles and gas. Drag force is proportional to the relative velocity of dust and gas components. However, the effect of this exchange of momentum is much stronger on the dust component simply because the mass of gas is much larger than the total mass of dust particles. Dynamics of dust particles in a protoplanetary disc are not necessarily the same as those of the gas component. They rotate more slowly than the local Keplerian velocity because of the pressure gradient which acts opposite to the direction of the central gravitational force. But an individual particle does not accelerate by the pressure gradient when its internal density is much larger than gas density and thereby dust particles rotate at their full Keplerian velocity.

Although a few authors have already studied gravitational stability of accretion discs consisting of dust particles and gas (e.g., Coradini et al. 1981; Noh et al. 1991), during recent years specific types of instabilities have been identified for clumping of dust particles in protoplanetary discs which are actually driven by the movement of dust particles through the gas (e.g., Youdin & Goodman 2005; Youdin & Lithwick 2007; Jacquet et al. 2011; Armitage 2011; Laibe & Price 2014) or dust-gas interaction (e.g., Sekiya 1983; Shariff & Cuzzi 2011; Youdin 2011). Streaming instability has been studied by many authors during recent years in the linear regime and its nonlinear evolution investigated via direct numerical simulations.

Drag driven instability is known as secular gravitational instability which is actually the dissipative version of classical gravitational instability for a dust layer in a fixed background gas component. Dynamics of the dust particles are mostly affected by gas-dust friction driven instabilities. Irrespective of the strength of the self-gravity, this instability is unconditional and can give raise to clumping of dust particles. There are simple theoretical explanations for this trend as have been clarified by Goodman & Pindor (2000) and Shariff & Cuzzi (2011). Radial perturbation leads to concentric rings of dust particles with slightly larger density compared to their ambient dust density. Particles at the outer edge of a ring feel larger gravitational force due to the accumulated mass of the ring and thereby will rotate faster. Since the drag force is proportional to velocity, inflow of dust particles increases at the outer edge of the ring. At the inner edge, the particles are orbiting at less than the Keplerian velocity because of the extra outward gravitational force. Thus, the particles will therefore be energized

by gas drag and will drift toward the ring. No matter how weak self-gravity is, the mentioned process will eventually give rise to clumping of dust particles.

Most of the previous linear studies of secular gravitational instability assume that dust particles are moving in a fixed background gaseous component (e.g., Shariff & Cuzzi 2011; Youdin 2011; Michikoshi et al. 2012; Shadmehri 2016). In these models, dust grains are treated as *pressure-less fluid*. The nondimensional gas friction time or dimensionless stopping time, which are defined as the product of the gas friction time and the Keplerian angular velocity, determines gas-dust coupling via the drag force. When dimensionless stopping time is greater than unity, dust particles are decoupled from the gas component and it would not be adequate to describe their dynamics using a fluid approximation (e.g., Jalali 2013).

Neglecting gas dynamics is justified by the fact that the total mass of dust particles is much smaller than the mass of the gaseous component of the disc and so only dynamics of dust particles are modified because of drag force. Although this argument seems to be reasonable, just recently Takahashi & Inutsuka (2014) showed that long-wavelength perturbations are stable when the dynamical feedback from dust grains in the gas component is considered. Their analysis implies that we cannot neglect small terms in the equation of motion for small growth rates. Thus, any physical agent that can modify gas dynamics may also affect dust dynamics indirectly via the drag force. Considering the important role of magnetic fields in the structure of protoplanetary discs, it is our motivation to study gravitational instability of a dust layer in a *magnetized* gaseous disc which has not been studied before to the best of our knowledge.

The structure of a protoplanetary disc strongly depends on the level of ionization and magnetic fields. External ionization sources such as X-ray radiation from the central star and cosmic rays can efficiently ionize surface layers of a disc. Most regions of a protoplanetary disc are weakly ionized, however, which implies that the coupling between the disc material and the magnetic field is incomplete. This will eventually lead to non-ideal MHD effects which appear because of the drift velocity between neutral particles and ionized species. There are three non-ideal MHD effects, i.e. the Ohmic resistivity, Hall effect and ambipolar diffusion. When the density is high and the ionization is very low, the Ohmic term is dominant, but the ambipolar diffusion term influences in the opposite limit. Between these extreme cases, the Hall term plays a significant role. All these non-ideal terms not only significantly modify the growth rate of magnetorotational instability (MRI) and its non-linear evolution, but also the dynamical structure of the disc and the launching of winds and outflows are affected by these effects. In this study, we neglect the possible role of non-ideal effects for simplicity. An important mechanism for transporting angular momentum in an accretion disc which leads to accretion is known as MRI and it operates in weakly ionized discs (Balbus & Hawley 1991). Magnetic fields may also provide an efficient mechanism for launching jets or outflows from a disc. Moreover, dynamical structure of a disc is significantly modified in the presence of magnetic fields. Gravitational stability of an accretion disc in the presence of a magnetic field has also been studied by many authors (e.g., Elmegreen 1989; Gammie 1996b; Fan & Lou 1997; Lizano et al. 2010; Lin 2014). Many previous studies concentrated on analyzing gravitational stability of purely gaseous discs and did not consider dynamics of the dust particles explicitly. Lizano et al. (2010) extended the classical Toomre criterion to a magnetized disc by introducing a modified Toomre parameter which should be greater than one for a gravitationally stable disc. They showed that magnetic tension and pressure stabilize the disc against axisymmetric gravitational perturbations which means magnetic fields suppress gravitational instability in protoplanetary discs.

In our study, we consider a disc consisting of magnetized gas and dust where they are coupled via drag force and the particle-to-gas feedback is included. We then explore possible effects of magnetic fields on gravitational stability of the dust layer using a linear perturbation analysis. In the next section, main assumptions and the basic equations of the model are presented. Linearized equations and the resulting dispersion relation are obtained in Section 3. Numerical analysis of the unstable modes and their dependence on the input parameters including strength of the magnetic field are presented in Section 4. We conclude with a summary of the results.

2 GENERAL FORMULATION

We consider a protoplanetary disc around a central star with mass M as a system consisting of gas and dust components undergoing momentum exchange. It is assumed that the disc is so thin that the motion of both gas and dust fluids are in the plane of the disc. It means that we do not consider vertical motion of dust particles. Previous linear studies of drag-driven instability in a dust layer have been done in the shearing sheet approximation (Goldreich & Lynden-Bell 1965). Here, we do not follow this approach. Our linear analysis is performed in cylindrical coordinates (r, ϕ, z) where the central star is located at its origin and time-evolution of the perturbations with wavelengths much smaller than the radial distance (i.e., the WKB approximation) is studied. Our basic equations for the gas component are similar to Lizano et al. (2010) who studied gravitational stability of a thin and magnetized accretion disc. However, we include the drag force due to the interaction with the dust fluid. Since we assume the dust particles are neutral, they do not feel magnetic force.

Thus, basic equations for the gas component are

$$\frac{\partial \Sigma}{\partial t} + \nabla \cdot (\Sigma \boldsymbol{w}) = 0, \tag{1}$$

$$\Sigma\Big(\frac{\partial \boldsymbol{w}}{\partial t}+\boldsymbol{w}\cdot\nabla\boldsymbol{w}\Big)=-\Sigma\nabla\Big(\Phi-\frac{GM}{r}\Big)-c_{\rm s}^2\nabla\Sigma +\frac{1}{4\pi}\int \boldsymbol{J}\times\boldsymbol{B}dz+\frac{\Sigma_{\rm d}(\boldsymbol{w}_d-w)}{t_{\rm stop}}, \quad (2)$$

$$\frac{\partial \boldsymbol{B}}{\partial t}=\nabla\times(\boldsymbol{w}\times\boldsymbol{B}), \quad (3)$$

$$\nabla\cdot\boldsymbol{B}=0, \quad (4)$$

where Σ, $\boldsymbol{w}$ and $c_{\rm s}$ are surface density, velocity and the sound speed of gas, respectively. Also, $t_{\rm stop}$ is the stopping time (see later text for its definition). It is assumed that the gas is isothermal. The magnetic field of gas is denoted by $\boldsymbol{B}$ and the current density is $\boldsymbol{J}=\nabla\times\boldsymbol{B}$. Note that Φ is the gravitational potential due to both gas and dust fluids. Note that the equations are integrated perpendicularly to the disc so that vertically averaged physical quantities do not depend on the vertical coordinate z.

Also, the basic equations describing the dust fluid are written as

$$\frac{\partial \Sigma_{\rm d}}{\partial t}+\nabla\cdot(\Sigma_{\rm d}\boldsymbol{w_d})=D\nabla^2\Sigma_{\rm d}, \quad (5)$$

$$\Sigma_{\rm d}\Big(\frac{\partial \boldsymbol{w}_d}{\partial t}+\boldsymbol{w}_d\cdot\nabla\boldsymbol{w}_d\Big) = -\Sigma_{\rm d}\nabla\Big(\Phi-\frac{GM}{r}\Big) +\frac{\Sigma_{\rm d}\Big(\boldsymbol{w}-\boldsymbol{w}_{\rm d}\Big)}{t_{\rm stop}}, \quad (6)$$

where $\boldsymbol{w}_{\rm d}$ is dust velocity and D is the radial diffusivity of the dust component because of the gas turbulence. The diffusion of dust particles due to stochastic forcing by gas turbulence has been studied by many authors (e.g., Youdin & Lithwick 2007). According to equation (36) of Youdin & Lithwick (2007), the radial diffusion coefficient D is written as

$$D=\frac{1+\tau+4\tau^2}{(1+\tau^2)^2}D_{\rm g}, \quad (7)$$

where $D_{\rm g}$ is the strength of turbulent diffusion in the gas which can be defined as

$$D_{\rm g}=\alpha c_{\rm s}^2\Omega^{-1}, \quad (8)$$

where α is the dimensionless measure of turbulent intensity. Strength of dust diffusion is measured by the dimensionless diffusivity coefficient ξ as $\xi=D/(c_{\rm s}^2\Omega^{-1})$. Moreover, τ is the dimensionless stopping time (see below). We note that the equation of continuity with the diffusion term is not commonly used. In fact, one can start from the Boltzmann equation to obtain the above hydrodynamical equations which leads to viscosity in the equation of motion instead of the diffusion term in the equation of continuity. Following previous works (e.g., Takahashi & Inutsuka 2014) we also used this problematic formulation, although these aspects of the work need further studies.

In the above equations, $t_{\rm stop}$ is the stopping time which is a time-scale for decay of relative velocity between the gas and the dust due to the drag force. We can then define nondimensional stopping time $\tau=t_{\rm stop}\Omega_{\rm K}$ (e.g., Miyake et al. 2016), where the angular Keplerian velocity is $\Omega_{\rm K}=\sqrt{GM/r^3}$. If we assume that all dust particles are spherical with the same radius a and have the same homogeneous internal density $\rho_{\rm m}$, then the nondimensional stopping time becomes $\tau=[\rho_{\rm m}a/(\rho_{\rm g}c_{\rm s})]\Omega_{\rm K}$ where $\rho_{\rm g}$ is the gas density. Note that this relation is valid when the size of the particles is smaller than the mean free path of the gas. For instance, in the minimum mass solar nebula (MMSN) model of Hayashi (1981) at radial distances larger than 1 AU from the central star with one solar mass, the mean free path of gas is larger than 1 cm which implies that the above relation for the stopping time is applicable to particles smaller than this length. Physical properties of the disc and dust distribution depend on the vertical location as well. However, we do not consider vertical variation of the physical quantities and one can then evaluate the nondimensional stopping time at the midplane of MMSN (Miyake et al. 2016)

$$\tau=1.8\times10^{-7}\left(\frac{a}{1\mu{\rm m}}\right)\left(\frac{r}{1{\rm AU}}\right)^{\frac{3}{2}}. \quad (9)$$

The internal density of a dust particle is assumed to be $\rho_{\rm m}=2$ g cm^{-3} and the surface density and sound speed obey power-law functions of the radial distance (Hayashi 1981):

$$\Sigma(r)=1.7\times10^3\left(\frac{r}{1{\rm AU}}\right)^{-\frac{3}{2}}{\rm g\,cm^{-2}}, \quad (10)$$

$$c_{\rm s}(r)=1.0\times10^5\left(\frac{r}{1{\rm AU}}\right)^{-\frac{1}{4}}{\rm cm\,s^{-1}}. \quad (11)$$

Note that our study is a *local* linear perturbation analysis based on the WKB approximation which means that we do not consider radial dependence of the initial equilibrium state. However, the above physical profiles specify how properties of a disc can vary with the radial distance. It can then be used to calculate the growth rate of unstable modes at a certain radial distance. As for the initial magnetic field, we assume the disc is threaded by a net large-scale vertical field $B_{\rm z0}$ so that the ratio of gas pressure to magnetic pressure β at the midplane of the disc is uniform throughout the disc. We then have

$$B_{\rm z0}(r)=590\left(\frac{\beta}{1000}\right)^{-\frac{1}{2}}\left(\frac{r}{1{\rm AU}}\right)^{-\frac{13}{8}}{\rm mG}. \quad (12)$$

Finally, our system of equations is closed by including the Poisson equation for a thin disc which is written as

$$\nabla^2\Phi=4\pi G(\Sigma+\Sigma_{\rm d})\delta(z). \quad (13)$$

Here, gravitational potential Φ due to both the gas and dust components is considered.

Lizano et al. (2010) studied gravitational instability of a gaseous magnetized disc but without dust particles. They vertically averaged all basic equations including the Lorentz term in the equation of motion. We generalize their

final main equations to produce a magnetized vertically averaged set of equations that include dust particles and their momentum exchange with the gas component.

Thus, the continuity equation for the gas is

$$\frac{\partial \Sigma}{\partial t}+\frac{1}{r}\frac{\partial}{\partial r}(r\Sigma u)+\frac{1}{r}\frac{\partial}{\partial \varphi}(\Sigma v)=0, \qquad (14)$$

where u and v are the radial and azimuthal components of gas velocity $\boldsymbol{w}$. The components of radial and azimuthal Lorentz force are

$$\begin{aligned}\int_{-H}^{H}\boldsymbol{J}\times\boldsymbol{B}dz \;=\; &\int_{-H}^{H}\Big[\Big(B_z\frac{\partial B_r}{\partial z}-B_z\frac{\partial B_z}{\partial r}\\ &-\frac{B_\varphi}{r}\frac{\partial (rB_\varphi)}{\partial r}+\frac{B_\varphi}{r}\frac{\partial B_r}{\partial \varphi}\Big)\boldsymbol{e}_r\\ &-\Big(\frac{B_z}{r}\frac{\partial B_z}{\partial \varphi}-B_z\frac{\partial B_\varphi}{\partial z}-\frac{B_r}{r}\frac{\partial (rB_\varphi)}{\partial r}\\ &+\frac{B_r}{r}\frac{\partial B_r}{\partial \varphi}\Big)\boldsymbol{e}_\varphi\Big]dz, \qquad (15)\end{aligned}$$

where $\boldsymbol{e}_r$ and $\boldsymbol{e}_\varphi$ are unit vectors in the radial and the azimuthal directions, respectively. We assume the toroidal component of the magnetic field is negligible, i.e. $B_\varphi=0$. This assumption not only simplifies the main equations, but it also prevents emergence of MRI modes in our analysis. In order to understand the dynamics in a magnetized disc, we note that MRI has a vital role. However, our purpose is to illustrate and understand the basic mechanism of secular gravitational instability with a magnetic field in the absence of MRI modes. Then the components of the Lorentz force become

$$\begin{aligned}\frac{1}{4\pi}\int_{-H}^{H}(\boldsymbol{J}\times\boldsymbol{B})_r dz \;=\; &\frac{1}{4\pi}\int_{-H}^{H}B_z\frac{\partial B_r^+}{\partial z}dz\\ &-\frac{1}{4\pi}\int_{-H}^{H}B_z\frac{\partial B_z}{\partial r}dz, \qquad (16)\end{aligned}$$

and

$$\begin{aligned}\frac{1}{4\pi}\int_{-H}^{H}(\boldsymbol{J}\times\boldsymbol{B})_\varphi dz \;=\; &-\frac{1}{4\pi}\int_{-H}^{H}(\frac{B_z}{r}\frac{\partial B_z}{\partial \varphi}\\ &+\frac{B_r^+}{r}\frac{\partial B_r^+}{\partial \varphi})dz. \qquad (17)\end{aligned}$$

By integrating over z, we obtain

$$\frac{1}{4\pi}\int_{-H}^{H}(\boldsymbol{J}\times\boldsymbol{B})_r dz=\frac{B_zB_r^+}{2\pi}-\frac{H}{4\pi}\frac{\partial B_z^2}{\partial r}, \qquad (18)$$

and

$$\frac{1}{4\pi}\int_{-H}^{H}(\boldsymbol{J}\times\boldsymbol{B})_\varphi dz=-\frac{H}{4\pi r}\frac{\partial}{\partial \varphi}(B_r^{+2}+B_z^2). \qquad (19)$$

Components of the equation of motion for the gas are also written as

$$\begin{aligned}\Sigma\Big[\frac{\partial u}{\partial t}+u\frac{\partial u}{\partial r}+\frac{v}{r}\frac{\partial u}{\partial \varphi}-\frac{v^2}{r}\Big]=&-c_{\rm s}^2\frac{\partial \Sigma}{\partial r}-\Sigma\frac{\partial V}{\partial r}\\ &+\frac{B_zB_r^+}{2\pi}-\frac{H}{4\pi}\frac{\partial B_z^2}{\partial r}+\frac{\Sigma_{\rm d}(u_{\rm d}-u)}{t_{\rm stop}}, \qquad (20)\end{aligned}$$

and

$$\begin{aligned}\Sigma\Big[\frac{\partial v}{\partial t}+u\frac{\partial v}{\partial r}+\frac{v}{r}\frac{\partial v}{\partial \varphi}+\frac{uv}{r}\Big]=&-\frac{c_{\rm s}^2}{r}\frac{\partial \Sigma}{\partial \varphi}-\frac{1}{r}\Sigma\Big(\frac{\partial V}{\partial \varphi}\Big)\\ &-\frac{H}{4\pi r}\frac{\partial}{\partial \varphi}\Big(B_r^{+2}+B_z^2\Big)+\frac{\Sigma_{\rm d}(v_{\rm d}-v)}{t_{\rm stop}}. \qquad (21)\end{aligned}$$

The disc scale height is $H=c_{\rm s}/\Omega_{\rm K}$. Also, B_r^+ is the radial component of the magnetic field at the surface of the disc. Note that V is the gravitational potential due to the central star and the components of the disc itself, i.e. $V=-GM/r+\Phi$, where Φ satisfies Poisson's equation (13).

The induction equation becomes

$$-\frac{\partial B_z}{\partial t}+\frac{1}{r}\Big[\frac{\partial}{\partial r}(rB_zu)+\frac{\partial}{\partial \varphi}(B_zv)\Big]=0. \qquad (22)$$

The continuity equation for the dust fluid is

$$\begin{aligned}&\frac{\partial \Sigma_{\rm d}}{\partial t}+\frac{1}{r}\frac{\partial}{\partial r}(r\Sigma_{\rm d}u_{\rm d})+\frac{1}{r}\frac{\partial}{\partial \varphi}(\Sigma_{\rm d}v_{\rm d})=\\ &\qquad D\Big[\frac{1}{r}\frac{\partial}{\partial r}\Big(r\frac{\partial \Sigma_{\rm d}}{\partial r}\Big)+\frac{1}{r^2}\frac{\partial^2\Sigma_{\rm d}}{\partial \varphi^2}\Big], \qquad (23)\end{aligned}$$

and the components of the equation of motion for the dust fluid are

$$\begin{aligned}&\Sigma_{\rm d}\Big[\frac{\partial u_{\rm d}}{\partial t}+u_{\rm d}\frac{\partial u_{\rm d}}{\partial r}+\frac{v_{\rm d}}{r}\frac{\partial u_{\rm d}}{\partial \varphi}-\frac{v_{\rm d}^2}{r}\Big]=\\ &\qquad -\Sigma_{\rm d}\frac{\partial V}{\partial r}+\frac{\Sigma_{\rm d}(u-u_{\rm d})}{t_{\rm stop}}, \qquad (24)\end{aligned}$$

and

$$\begin{aligned}&\Sigma_{\rm d}\Big[\frac{\partial v_{\rm d}}{\partial t}+u_{\rm d}\frac{\partial v_{\rm d}}{\partial r}+\frac{v_{\rm d}}{r}\frac{\partial v_{\rm d}}{\partial \varphi}+\frac{u_{\rm d}v_{\rm d}}{r}\Big]=\\ &\qquad -\frac{\Sigma_{\rm d}}{r}(\frac{\partial V}{\partial \varphi})+\frac{\Sigma_{\rm d}(v-v_{\rm d})}{t_{\rm stop}}. \qquad (25)\end{aligned}$$

We note that dust particles are assumed to be neutral, and so they do not experience magnetic force. Moreover, our dusty fluid is pressure-less and, for this reason, the gradient of pressure does not appear in the above equation of motion.

3 LINEAR PERTURBATIONS

After deriving basic MHD equations including dust contributions, we can now perturb all physical quantities around a uniform equilibrium configuration and then investigate their fate provided that perturbations are much smaller than the initial state. This kind of linear analysis will lead to a dispersion relation to specify unstable modes and their growth rates. The subscripts 0 and 1 are used to denote the initial state and the perturbed quantities, respectively. Equilibrium states must satisfy continuity, motion and induction equations. We know that initial states are independent of t, φ and z and the velocities of dust and gas components are assumed to be same initially. We assume that

Σ_0 is independent of r. Moreover, we assume that the radial component of the magnetic field at the surface of the disc is negligible for simplicity. Also, the initial vertical component of the magnetic field is considered to be independent of the radial distance. Then, the equilibrium state satisfies all equations automatically except for the radial component of motion for gas and dust. The zeroth order of the radial component of equation of motion for the gas is

$$\Omega^2 r-\frac{c_{\rm s}^2}{\Sigma_0}\frac{\partial\Sigma_0}{\partial r}-\frac{\partial V_0}{\partial r}+\frac{B_{0r}^{+}B_{0z}}{2\pi\Sigma_0}-\frac{H}{4\pi\Sigma_0}\frac{\partial B_{0z}^2}{\partial r}=0, \quad (26)$$

which reduces to $\Omega^2 r-\frac{\partial V_0}{\partial r}=0$ subject to our mentioned simplifying assumptions.

Our linear perturbation of a physical quantity X is $X = X_0 + X_1 e^{{\rm i}(\omega t+kr-m\varphi)}$, where ω is the frequency, k is the radial wavenumber, m is a positive integer for nonaxisymmetric perturbations and $m = 0$ for axisymmetric modes. Here, we only consider axisymmetric perturbations. Following Lizano et al. (2010), we also make a further assumption that $|k|r \gg 1$, which means the wavelength of perturbations is much smaller than the radial distance.

Thus, the linearized dynamical equations for axisymmetric modes expand to

$$\omega\frac{\Sigma_1}{\Sigma_0}+ku_1=0, \quad (27)$$

$$i\omega u_1-2\Omega v_1+ikc_{\rm s}^2\frac{\Sigma_1}{\Sigma_0}+ikV_1+i(1+kH)\frac{B_{z0}B_{1z}}{2\pi\Sigma_0} -\frac{Z(u_{1d}-u_1)}{t_{\rm stop}}=0, \quad (28)$$

$$i\omega v_1+u_1\frac{\kappa^2}{2\Omega}-\frac{Z(v_{1d}-v_1)}{t_{\rm stop}}=0, \quad (29)$$

$$i\omega B_{1z}+ikB_{z0}u_1=0, \quad (30)$$

$$(i\omega+Dk^2)\frac{\Sigma_{1d}}{Z\Sigma_0}+iku_{1d}=0, \quad (31)$$

$$i\omega u_{1d}-2\Omega_K v_{1d}+ikV_1-\frac{(u_1-u_{1d})}{t_{\rm stop}}=0, \quad (32)$$

$$i\omega v_{1d}+u_{1d}\frac{\kappa^2}{2\Omega_K}-\frac{(v_1-v_{1d})}{t_{\rm stop}}=0, \quad (33)$$

$$V_1+\frac{2\pi G}{k}\left(\frac{\Sigma_1}{1+kH}+\frac{\Sigma_{1d}}{1+kH_{\rm d}}\right)=0, \quad (34)$$

where $H_{\rm d}$ is the dust scale height $H_{\rm d}=\sqrt{\frac{\alpha}{\tau}}H$ and Z is the ratio of the dust density to the gas density or disc metallicity for the initial state, i.e. $Z=\Sigma_{0d}/\Sigma_0$. Moreover, λ is the dimensionless mass-to-flux ratio and is defined as

$$\lambda=\frac{2\pi G^{\frac{1}{2}}\Sigma_0}{B_{z0}}. \quad (35)$$

The additional parameter resulting in our analysis is the magnetically modified Toomre parameter $Q_{\rm M}$, i.e.

$$Q_{\rm M}=\frac{\Theta^{\frac{1}{2}}c_{\rm s}\kappa}{\pi G\epsilon\Sigma_0}, \quad (36)$$

where $\Theta=1+\frac{B_{z0}^2 H}{2\pi c_{\rm s}^2\Sigma_0}$ and $\epsilon=1-\frac{1}{\lambda^2}$. Also, κ is the epicyclic frequency where in the absence of magnetic effects it becomes the Keplerian angular velocity. But magnetic forces reduce the epicyclic frequency, though its exact value depends on the geometry of the magnetic configuration. Lizano et al. (2010) approximated the epicyclic frequency as $\kappa=f\Omega$ where f is a number less than unity. Obviously, we can assume $f\simeq 1$ for weak magnetic fields.

If we introduce the nondimensional growth rate and the nondimensional wavenumber as $x=i\omega/\Omega$ and $y=kH$ respectively, then we can re-write the above linearized equations:

$$x\frac{\Sigma_1}{\Sigma_0}+i\frac{y}{c_{\rm s}}u_1=0, \quad (37)$$

$$\left[x+\frac{Z}{f\tau}+(\frac{2y(1+y)}{\lambda^2 x})\left(\frac{\Theta^{\frac{1}{2}}}{Q_M\epsilon}\right)\right]u_1-2v_1+ iyc_{\rm s}\frac{\Sigma_1}{\Sigma_0}+i\frac{y}{c_{\rm s}}V_1-\frac{Z}{f\tau}u_{1d}=0, \quad (38)$$

$$\left[x+\frac{Z}{f\tau}\right]v_1+\frac{1}{2}u_1-\frac{Z}{f\tau}v_{1d}=0, \quad (39)$$

$$xB_{1z}+i\frac{y}{c_{\rm s}}B_{z0}u_1=0, \quad (40)$$

$$[x+\xi y^2]\frac{\Sigma_{1d}}{Z\Sigma_0}+i\frac{y}{c_{\rm s}}u_{1d}=0, \quad (41)$$

$$\left[x+\frac{1}{f\tau}\right]u_{1d}-\frac{2}{f}v_{1d}+i\frac{y}{c_{\rm s}}V_1-\frac{u_1}{f\tau}=0, \quad (42)$$

$$\left[x+\frac{1}{f\tau}\right]v_{1d}+\frac{f}{2}u_{1d}-\frac{v_1}{f\tau}=0, \quad (43)$$

$$V_1+\frac{2\Theta^{\frac{1}{2}}c_{\rm s}^2}{Q_M\epsilon\Sigma_0 y}\left(\frac{\Sigma_1}{1+y}+\frac{\Sigma_{1d}}{1+\sqrt{\frac{\alpha}{\tau}}y}\right)=0. \quad (44)$$

Thus, we have eight equations and eight unknowns, i.e. Σ_1, $\Sigma_{1\rm d}$, v_1, u_1, $v_{1\rm d}$, $u_{1\rm d}$, V_1 and $B_{1\rm z}$. Since the above linearized equations are valid for perturbations with a wavelength much smaller than radial distance, i.e. $kr \gg 1$, we can consider perturbations which satisfy this inequality: $kH = y \gg H/r$. For instance, in a thin disc with $H/r = 0.1$, we only consider perturbations which are larger than this value, i.e. $y \gg 0.1$. In addition to this constraint on local approximation, the validity of the vertically integrated equations requires $ku < \Omega_{\rm K}$ (e.g., Wu & Li 1996; Kato et al. 1996). This requirement can be written as $kH < (\alpha H/r)^{-1}$ where α is the disc viscosity. Thus, our analysis is valid for $(H/r) \ll y < (\alpha H/r)^{-1}$. If we set $\alpha = 0.01$ and $H/r = 0.1$, then the valid range of nondimensional wavenumber becomes $0.1 \ll y < 10^3$. Also, the validity of vertically integrated equations implies

that the growth rates of the unstable modes are less than the angular velocity (Kato et al. 1996). This requirement is justified by the unstable modes as we will show.

Existence of a set of nontrivial solutions for the above linearized equations implies that the determinant of the coefficients becomes zero which gives us an algebraic equation involving the input parameters, growth rate and the wavenumber of the perturbations. Using MAPLE software, we found the dispersion relation. But the equation is very lengthy, so we do not include it here. However, our analysis is based on the roots of this equation which can be calculated numerically. Obviously, unstable modes correspond to the roots with a positive real part, i.e. $\mathrm{Re}(x) > 0$. We generally found one or two unstable modes for a given set of the input parameters.

It is useful to re-write the input parameters as follows (Lizano et al. 2010):

$$\lambda = 2.71\mu\Big(\frac{N_{\rm H}}{10^{24}{\rm cm}^2}\Big)\Big(\frac{B_{z0}}{1{\rm mG}}\Big)^{-1}, \qquad (45)$$

$$\Theta = 1 + 1.15\times10^{-2}\Big(\frac{B_{z0}}{1{\rm mG}}\Big)^{2}\Big(\frac{H}{1{\rm AU}}\Big) \times\Big(\frac{N_H}{10^{24}{\rm cm}^2}\Big)^{-1}\Big(\frac{T}{1{\rm K}}\Big)^{-1}, \qquad (46)$$

$$\epsilon = 1 - 1.36\times10^{-1}\Big(\frac{1}{\mu^2}\Big)\Big(\frac{B_{z0}}{\rm mG}\Big)^{2}\Big(\frac{N_{\rm H}}{10^{24}{\rm cm}^2}\Big)^{-2}, \qquad (47)$$

$$Q_M = 2.12\Big(\frac{\Theta^{\frac{1}{2}}}{\epsilon\mu^{\frac{3}{2}}}\Big)\Big(\frac{\Omega}{10^{-2}{\rm km\ s^{-1}\ AU^{-1}}}\Big) \times\Big(\frac{T}{1{\rm K}}\Big)^{\frac{1}{2}}\Big(\frac{N_{\rm H}}{10^{24}{\rm cm}^2}\Big)^{-1}, \qquad (48)$$

where μ is the molecular weight, $N_{\rm H}$ is the hydrogen column density, T is the gas temperature and Ω is the angular velocity.

4 ANALYSIS

We can now investigate axisymmetric unstable modes for different sets of input parameters in order to explore possible effects of the magnetic field on drag-driven instability. Nonzero values for m essentially do not affect behavior of the unstable solutions.

In Figures 1 and 2, we assume $H = 143\,{\rm AU}$, $T = 250$ K, $\mu = 2.33$ and $N_{\rm H} = 3.46\times10^{24}\,{\rm cm}^{-2}$ (Lizano et al. 2010). Corresponding to these input parameters, one can calculate the other parameters based on Equations (45)–(48) for different values of the initial vertical magnetic field (Table 1). We first examine the dependence of the growth rate on the grain size, or dimensionless stopping time.

Figure 1 shows unstable growth rate for particles with different sizes, ranging from strongly coupled particles with dimensionless stopping time $\tau = 5\times10^{-3}$ (top panel) and $\tau = 10^{-2}$ (middle panel) to a slightly less coupled

Table 1 Input Parameters for Different Values of the Initial Vertical Magnetic Field B_{z0}

$B_{z0}({\rm mG})$	λ	Θ	ϵ	f	Q_M
0	∞	1	1	1	1.99
5	4.35	1.05	0.94	1	2.16
10	2.17	1.21	0.78	1	2.79
15	1.45	1.48	0.52	1	4.9

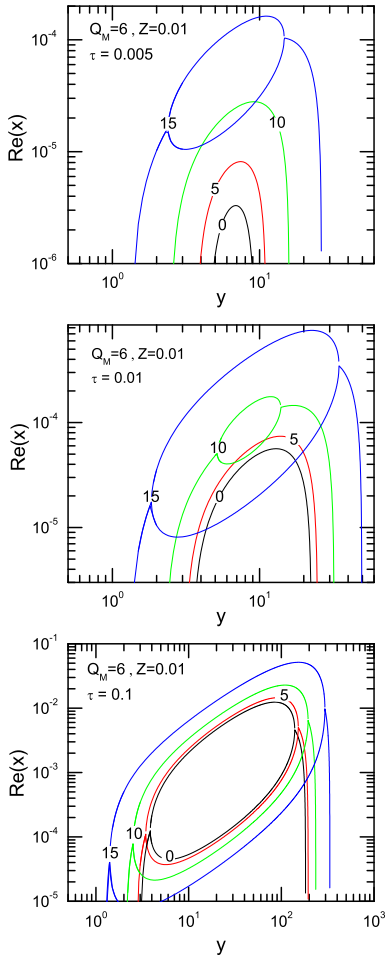

Fig. 1 Dispersion relation of the unstable modes for different values of magnetic strength and dimensionless stopping time. Each curve is labeled by its corresponding value of B_{z0}. Here, the magnetic Toomre parameter is $Q_M = 6$ which is larger than the threshold for instability (see Table 1).

case with $\tau = 10^{-1}$ (bottom panel). Each curve is labeled by its corresponding value of B_{z0}. In this figure, the standard value of disc metallicity is adopted, i.e. $Z = 0.01$, the Toomre parameter is $Q_M = 6$ and $\alpha = 10^{-6}$. Here, different values of τ are considered. Note that our adopted value of the Toomre parameter is greater than the threshold of instability which means that the system is stable in the absence of dust particles. For some of the input parameters, we found two unstable roots where one root is much smaller than the other one. We actually displayed both roots, though the larger root which specifies the most

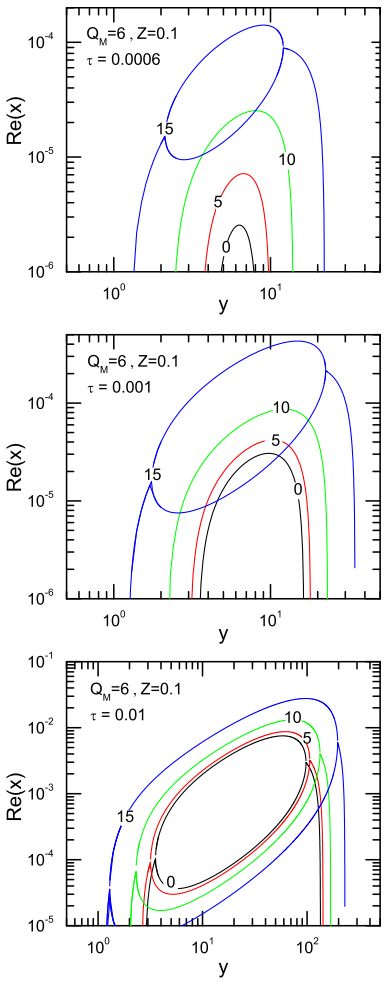

Fig. 2 Same as Fig. 1, but the surface density of dust particles is larger.

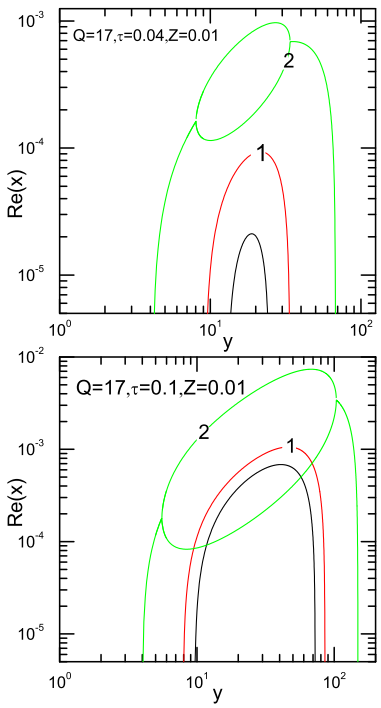

Fig. 3 Growth rate of the unstable modes as a function of the normalized wavenumber in the MMSN at the radial distance 100 AU where the Toomre parameter is $Q_M = 17$. Other input parameters are the same as those in previous figures, and different values for the dimensionless stopping time τ are adopted. Each curve is labeled by the corresponding value of the vertical magnetic field and the black curve is for the non-magnetized case. We found that for magnetic field strength larger than 2 mG, the parameter ϵ becomes negative which is not acceptable.

unstable root is more interesting. We consider different values of the disc metallicity (i.e., $Z = 0.01$ and $Z = 0.1$) in our analysis to explore possible effects of its variations on the instability.

Figure 1 shows that instability occurs in the presence of the magnetic fields, and as the strength of the magnetic field increases the instability grows faster. This feature is understandable by the fact that the critical value of the Toomre parameter for instability in the absence of dust particles increases with the magnetic field (see Table 1). Since we assume a fixed value for the Toomre parameter, the system becomes closer to the threshold of instability by increasing the magnetic field.

Figure 2 is the same as Figure 1, but the disc metallicity is larger, i.e. $Z = 0.1$. Again, the system is unstable in the presence of dust particles.

Figure 1 shows that when the disc contains aerodynamically well-coupled dust particles, even weak magnetic fields can considerably destabilize the system. For example, in the strongly coupled case (top panel), the system is unstable in the presence of the magnetic field. But as the level of dust-gas coupling reduces, the growth rate increases. Moreover, wavelength of the most unstable mode increases with the magnetic field strength when the particles are well-coupled to the gas. Note that in all cases, the corresponding modified Toomre parameter Q_M is larger than one (see Table 1).

Figure 3 shows growth rate of the instability in the MMSN at the radial distance 100 AU where the Toomre parameter is $Q_M = 17$. The rest of the input parameters are the same as previous figures. At the radial distance 100 AU, when we have $\tau = 0.04$, the size of the dust particles is $a = 222$ μm, the most unstable wavelength is around 1 AU and the corresponding growth time is 0.13×10^6 years. For $\tau = 0.1$, the size of the dust particles is $a = 555$ μm and the most unstable wavelength and the corresponding growth time become 2.45 AU and 10^6 years, respectively.

Cosmic rays and radiation from the central star are the main sources of ionization in a protoplanetary disc. It is known that there is a region in a protoplanetary disc where neither cosmic rays can penetrate to ionize the gas nor the radiation of the central star is able to ionize the gas. This non-ionized region which is magnetically *inactive* is called a dead zone (Gammie 1996a). But interior to the dead zone or beyond that region, the gaseous component of the disc is magnetically active. Our analysis shows that drag-driven

instability is more efficient in the magnetized regions compared to the regions where magnetic fields do not play a significant role. Although the numerical values adopted in previous figures are certainly subject to uncertainties, our analysis serves as a proof of concept to illustrate the important role of the magnetic field in drag-driven instability in protoplanetary discs.

5 CONCLUSIONS

We surveyed linear instability of a dust layer in a magnetized gaseous disc for perturbations with wavelengths much smaller than the radial distance. One of the interesting findings in this paper is that the magnetic field can amplify instability for even a weak gas-dust coupling. In particular, we showed that for well-coupled particles, even a weak magnetic field is able to amplify the instability and leads to a completely unstable system. Our study shows that the greatest response for axisymmetric perturbations occurs at large wavelengths. We also found that in the presence of magnetic fields, enhancing the disc metallicity promotes instability because this enhancement leads to stronger self-gravity of particles and slower radial drift.

The time-scale of drag driven instability should be shorter than the radial drift time-scale if the instability is responsible for planetesimal formation. Based on this physical constraint, the minimum dust abundance for planetesimal formation via secular gravitational instability has been estimated by Takeuchi & Ida (2012). Considering the destabilizing role of the magnetic field, however, we think this minimum dust abundance is modified if magnetic fields are considered.

Acknowledgements We are very grateful to the anonymous referee for his/her very useful comments and suggestions which greatly helped us to improve the paper. MS is grateful to Prof. Shu-ichiro Inutsuka for his useful comments on the early version of this manuscript.

References

Armitage, P. J. 2011, ARA&A, 49, 195
Balbus, S. A., & Hawley, J. F. 1991, ApJ, 376, 214
Chiang, E., & Youdin, A. N. 2010, Annual Review of Earth and Planetary Sciences, 38, 493
Coradini, A., Magni, G., & Federico, C. 1981, A&A, 98, 173
Elmegreen, B. G. 1989, ApJ, 342, L67
Fan, Z., & Lou, Y.-Q. 1997, MNRAS, 291, 91
Gammie, C. F. 1996a, ApJ, 457, 355
Gammie, C. F. 1996b, ApJ, 462, 725
Gammie, C. F. 2001, ApJ, 553, 174
Goldreich, P., & Lynden-Bell, D. 1965, MNRAS, 130, 125
Goodman, J., & Pindor, B. 2000, Icarus, 148, 537
Hayashi, C. 1981, Progress of Theoretical Physics Supplement, 70, 35
Jacquet, E., Balbus, S., & Latter, H. 2011, MNRAS, 415, 3591
Jalali, M. A. 2013, ApJ, 772, 75
Kato, S., Abramowicz, M. A., & Chen, X. 1996, PASJ, 48, 67
Laibe, G., & Price, D. J. 2014, MNRAS, 444, 1940
Lin, M.-K. 2014, ApJ, 790, 13
Lizano, S., Galli, D., Cai, M. J., & Adams, F. C. 2010, ApJ, 724, 1561
Matzner, C. D., & Levin, Y. 2005, ApJ, 628, 817
Michikoshi, S., Kokubo, E., & Inutsuka, S.-i. 2012, ApJ, 746, 35
Miyake, T., Suzuki, T. K., & Inutsuka, S.-i. 2016, ApJ, 821, 3
Noh, H., Vishniac, E. T., & Cochran, W. D. 1991, ApJ, 383, 372
Rafikov, R. R. 2005, ApJ, 621, L69
Sekiya, M. 1983, Progress of Theoretical Physics, 69, 1116
Shadmehri, M. 2016, ApJ, 817, 140
Shariff, K., & Cuzzi, J. N. 2011, ApJ, 738, 73
Takahashi, S. Z., & Inutsuka, S.-i. 2014, ApJ, 794, 55
Takeuchi, T., & Ida, S. 2012, ApJ, 749, 89
Wu, X.-B., & Li, Q.-B. 1996, ApJ, 469, 776
Youdin, A. N. 2011, ApJ, 731, 99
Youdin, A. N., & Goodman, J. 2005, ApJ, 620, 459
Youdin, A. N., & Lithwick, Y. 2007, Icarus, 192, 588